A numerical study on a V-shaped laminar stratified flame, Paper No. IMECE2005-79607

Guo, H.; Smallwood, Gregory; Galizzi, C.; Escudié, C.

Publisher's version / Version de l'éditeur:

Proceedings of IMECE2005, 2005 ASME International Mechanical Engineering Congress and Exposition, 2005

Proceedings of IMECE2005
2005 ASME International Mechanical Engineering Congress and Exposition
November 5-11, 2005, Orlando, Florida USA

IMECE2005-79607

A NUMERICAL STUDY ON A V-SHAPED LAMINAR STRATIFIED FLAME

Hongsheng Guo
Institute for Chemical Process and Environmental Technology, National Research Council of Canada
1200 Montreal Road, Ottawa, Ontario, Canada K1A 0R6
Fax: (613)957-7869, phone: (613)991-0869
Email: hongsheng.guo@nrc-cnrc.gc.ca

Gregory J. Smallwood
Institute for Chemical Process and Environmental Technology, National Research Council of Canada
1200 Montreal Road, Ottawa, Ontario, Canada K1A 0R6
Fax: (613)957-7869, phone: (613)993-1391
Email: greg.smallwood@nrc-cnrc.gc.ca

Cedric GALIZZI
CETHIL Centre de Thermique de Lyon
UMR 5008 CNRS – INSA – UCBL
INSA de Lyon – 9, rue de la Physique – 69621
Villeurbanne Cedex - France
Fax: + (33) 4 72 43 88 11, phone: + (33) 4 72 43 70 41
Email: cedric.galizzi@insa-lyon.fr

Dany Escudié
CETHIL Centre de Thermique de Lyon
UMR 5008 CNRS – INSA – UCBL
INSA de Lyon – 9, rue de la Physique – 69621
Villeurbanne Cedex - France
Fax: + (33) 4 72 43 88 11, phone: + (33) 4 72 43 70 41
Email: dany.escudie@insa-lyon.fr

ABSTRACT

A V-shaped laminar stratified flame was investigated by numerical simulation. The primitive variable method, in which the fully elliptic governing equations were solved with detailed chemistry and complex thermal and transport properties, was used.

The results indicate that in addition to the primary premixed flame, the stratified charge in a combustor causes the formation of a diffusion flame. The diffusion flame is located between the primary premixed flame branches. The fuel is fully decomposed and converted to some intermediate species, like CO and H_2, in the primary premixed flame branches. Due to the shortage of oxygen, the formed CO and H_2 in the fuel rich region of the premixed flame branch is further transported to the downstream until they meet the oxygen from the fuel lean region. This leads to the formation of the diffusion flame. There is an interaction between the diffusion flame and the primary premixed flame branches. The interaction intensifies the burning speed of the primary premixed flame. Both the heat transfer and the diffusion of hydrogen and some radicals cause the interaction. With the increase of the stratified charge region, the diffusion flame zone is enlarged and the interaction is enhanced.

Keywords: laminar flame, stratified combustion, triple flame, direct injection.

INTRODUCTION

Direct injection spark ignited gasoline engine technique has been quickly developed in past few years, due to its higher fuel efficiency and lower green-house gas emission. Inside the cylinder of a direct injection spark ignited engine, a stratified charge near the spark plug is usually generated. The combustion inside a spark ignited engine is much more complex than in a homogeneous charge engine.

Many previous studies [1-4] on stratified charge combustion were devoted to industrial configurations where the fundamental mechanisms of stratified combustion could not be easily understood. Fundamental studies [5, 6] adopting ideal flame configurations and direct numerical simulations [7, 8] showed that the characteristics of the flame propagation in a stratified mixture are different from those in a homogeneous mixture. The flame speed in a stratified field is increased compared to in a homogeneous field.

Galizzi [9] experimentally studied a V-shaped flame stabilized in a field with stratified fuel-air ratio. A particular shape of the flame front, called "peninsula", was observed in the experiment. However, the mechanism for this flame "peninsula" was not properly explained.

In this paper, the flame that Galizzi [9] experimentally investigated was numerically simulated by detailed chemistry and complex thermal and transport properties. The purpose is to use the details from numerical simulation to understand the specific flame structure observed by Galizzi [9]. The flame propagation speed in a stratified field will also be investigated and compared with that in a homogeneous field.

NUMERICAL MODEL

Since the flame size investigated in [9] is too big to simulate by the current computer, the dimension was reduced to one fifth of the original flame in the simulation of this paper.

As a result, most parameters were decreased to one fifth of those in the experiment, except the inlet temperature. However, to verify the effect of the reduction in flame dimension and parameters on the results, two additional simulations were carried out.

Figure 1a shows the flame configuration used in the simulations. A 2.8 x 3.0 cm^2 two-dimensional rectangular domain was used. The bottom side is the inlet, and the upper side is the outlet. A solid rod was put at the inlet to stabilize the flame. In the normal simulation (Flame 1), the diameter of the solid rod, the distance (L) between the solid rod and the origin of the coordinate system (the middle point of the bottom side, x = 0.0) and the inlet velocity were, respectively, reduced to one fifth of those in the experiment. These three parameters used in the normal simulation are 0.4 mm, 0.4 mm and 100 cm/s. However the inlet temperature was kept the same as that in the experiment, i.e. 300 K. The temperature of the rod was not measured in the experiment. A value of 1500 K was used in the simulation.

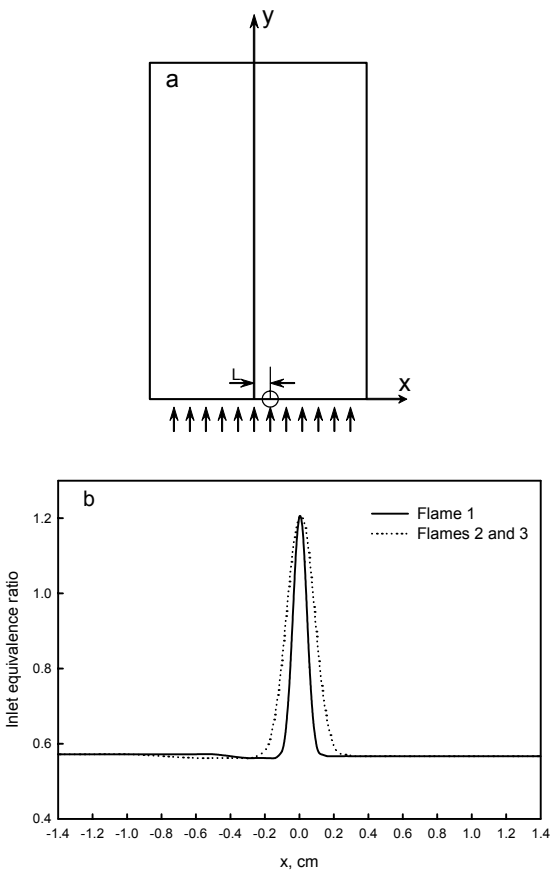

Fig. 1 Flame configuration and inlet equivalence ratio distributions. a. Flame configuration; b. Equivalence ratio.

In the first additional simulation (Flame 2), everything is the same as that in Flame 1, except that the inlet equivalence radio profile was changed, as given in Fig. 1b. The distance between the solid rod and the origin of the coordinate system was changed to 0.8 mm, while other conditions are the same as those in Flame 2 for the second additional simulation (Flame 3).

The fluid entering the domain was methane/air mixture. The equivalence ratio varied along x direction at the inlet. As a result of the reduction in the dimension of the flame, the stratified charge range (width in x direction) was proportionally reduced to 20% and 40% of that in the experiment [9], respectively, for Flame 1 and Flames 2 and 3. The distributions of the inlet equivalence ratio for the three simulated flames are shown in Fig. 1b.

The numerical model solved fully elliptic governing equations for the conservation of mass, momentum, energy and chemical species. The governing equations are [10]

Continuity:

$$\frac{\partial}{\partial x}(\rho u)+\frac{\partial}{\partial y}(\rho v)=0 \tag{1}$$

Momentum:

$$\rho u\frac{\partial u}{\partial x}+\rho v\frac{\partial u}{\partial y}=-\frac{\partial p}{\partial x}+2\frac{\partial}{\partial x}\left(\mu\frac{\partial u}{\partial x}\right)+\frac{\partial}{\partial y}\left(\mu\frac{\partial u}{\partial y}\right)-\frac{2}{3}\frac{\partial}{\partial x}\left(\mu\frac{\partial u}{\partial x}\right)-\frac{2}{3}\frac{\partial}{\partial x}\left(\mu\frac{\partial v}{\partial y}\right)+\frac{\partial}{\partial y}\left(\mu\frac{\partial v}{\partial x}\right) \tag{2}$$

$$\rho u\frac{\partial v}{\partial x}+\rho v\frac{\partial v}{\partial y}=-\frac{\partial p}{\partial y}+2\frac{\partial}{\partial y}\left(\mu\frac{\partial v}{\partial y}\right)+\frac{\partial}{\partial x}\left(\mu\frac{\partial v}{\partial x}\right)-\frac{2}{3}\frac{\partial}{\partial y}\left(\mu\frac{\partial u}{\partial x}\right)-\frac{2}{3}\frac{\partial}{\partial y}\left(\mu\frac{\partial v}{\partial y}\right)+\frac{\partial}{\partial x}\left(\mu\frac{\partial u}{\partial y}\right)-\rho g \tag{3}$$

Energy:

$$c_p\left(\rho u\frac{\partial T}{\partial x}+\rho v\frac{\partial T}{\partial y}\right)=\frac{\partial}{\partial x}\left(\lambda\frac{\partial T}{\partial x}\right)+\frac{\partial}{\partial y}\left(\lambda\frac{\partial T}{\partial y}\right)-\sum_{k=1}^{KK}\left[\rho c_{pk}Y_k\left(V_{kx}\frac{\partial T}{\partial x}+V_{ky}\frac{\partial T}{\partial y}\right)\right]-\sum_{k=1}^{KK}h_kW_k\omega_k+q_r \tag{4}$$

Chemical species:

$$\rho u\frac{\partial Y_k}{\partial x}+\rho v\frac{\partial Y_k}{\partial y}=-\frac{\partial}{\partial x}(\rho Y_kV_{kx})-\frac{\partial}{\partial y}(\rho Y_kV_{ky})+W_k\omega_k\ ,$$

$$k=1,\ 2,\ \ldots,\ KK \tag{5}$$

where u and v are the velocities in x and y directions, respectively; T the temperature of the mixture; ρ the density of the mixture; W_k the molecular weight of the kth species; λ the mixture thermal conductivity; c_p specific heat of the mixture under constant pressure; c_{pk} specific heat of the kth species under constant pressure; ω_k mole production rate of the kth species per unit volume. Quantity h_k denotes the specific enthalpy of the kth species; g the gravitational acceleration which was in the vertical (y) direction; μ the viscosity of the mixture; Y_k the mass fraction of the kth species; V_{kx} and V_{ky} the diffusion velocities of the kth species in x and y directions; and

KK the total species number. The set of governing equations was closed by the ideal gas state equation.

The last term on the right hand side of Eq.4, q_r, is the source term due to radiation heat transfer. It was obtained by the discrete ordinate method coupled to a statistical narrow-band correlated-K (SNBCK) based wide band model for the properties of CO, CO_2 and H_2O [11].

The species diffusion velocity consists of three terms: ordinary diffusion, thermal diffusion and correction diffusion velocities, i.e.

$$V_{kx_i} = V_{okx_i} + V_{Tkx_i} + V_{cx_i}, \quad k=1,2,\ldots,KK, \qquad x_i=x, y, \qquad (6)$$

The ordinary diffusion velocity, V_{okx_i}, and the thermal diffusion velocity, V_{Tkx_i}, were respectively calculated by the approximate mixture-average formulation and the accurate multi-component formulation [12]. The correction diffusion velocity, V_{cx_i}, was introduced to ensure the net diffusive flux of all species to be zero.

Low Mach number flow was assumed, and hence the pressure field only affects the velocity field. The governing equations were discretized using the control volume method. The SIMPLE numerical scheme [13] was used to deal with the pressure and velocity coupling. The diffusion and convective terms in the conservation equations were respectively discretized by the central and upwind difference methods. A 358 × 224 cell mesh was used, with finer resolution in the primary reaction zone, where the grid size was 0.05 mm × 0.05 mm. The discretized equations of species mass fraction were solved simultaneously for every cell to accelerate the convergence process [14], while those of momentum, energy and pressure correction were solved sequentially using the tri-diagonal matrix algorithm (TDMA).

The free slip boundary condition was used for the left and right hand side boundaries, and zero gradient condition was used for the outlet (the upper boundary). The inlet species concentrations were specified according to the local equivalence ratio, as in Fig. 1b.

The chemical reaction mechanism used is GRI-Mech 3.0 [15], with the removal of all the reactions and species related to NO_X formation. The revised reaction scheme consists of 36 species and 219 reactions. The thermal and transport properties were obtained by using the database of GRI-Mech 3.0 and the algorithms given in [12, 16].

RESULTS AND DISCUSSION

For the sake to present and explain the results, the tomography of the V-shaped stratified flame obtained by Galizzi [9] experimentally is illustrated in Fig. 2. A V-shaped flame was stabilized around a rod. A particular shape, the "peninsula", was clearly observed along the left V branch. The purpose of this paper is to understand what this particular peninsula is, and how it affects the flame speed along the front of the V-shaped flame.

Figure 3 shows the distributions of heat release rate in the three simulated flames. It is observed that there is a V-shaped heat release region in each flame. This reflects the primary reaction zone. The bottom of the V is at the position where the stabilization rod is located. This can be easily understood, since the inlet velocity (100 cm/s) is much higher than the maximum flame speed of CH_4/air mixture (40 cm/s) and the flame was stabilized because of the rod.

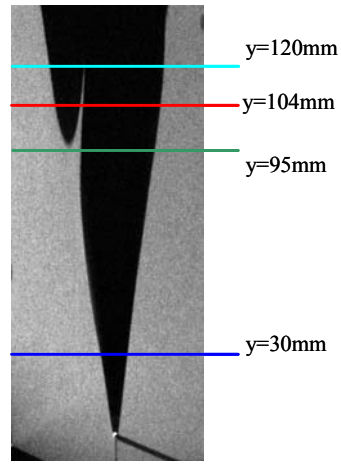

Fig. 2 Tomography of the V-shaped stratified laminar flame observed by Galizzi [9].

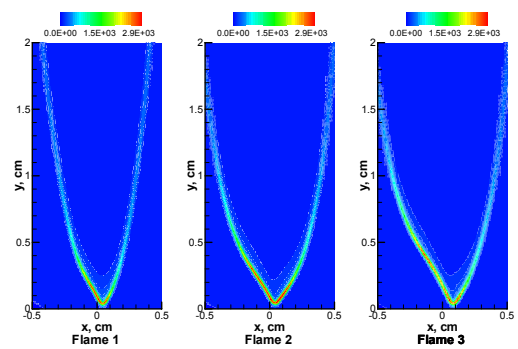

Fig. 3 Heat release rate (Joules/cm^{3}s) in the simulated flames.

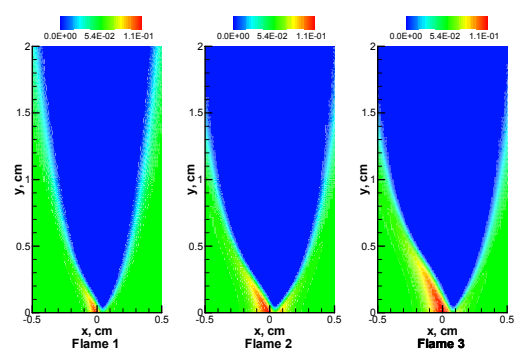

Fig. 4 CH_4 mole fraction in the simulated flames.

Figure 4 illustrates the distribution of the parent fuel, CH_4, in the three simulated flames. A V-shaped fuel-free zone is formed for each simulated flame. This indicates that after entering the domain from the bottom, the parent fuel was consumed or decomposed along the primary V-shaped reaction

zone. However, no particular peninsula like that shown in Fig. 2 can be found from the distribution of fuel.

Figure 5 displays the distributions of two intermediate species, H_2 and CO, in the three flames. It is demonstrated that there is a V-shaped zone with higher concentrations of CO and H_2 for each flame. The V-shaped region with higher concentrations of CO and H_2 corresponds to the primary reaction zone in Fig. 3. This phenomenon implies that the parent fuel is first quickly converted to the intermediate species H_2 and CO in the primary reaction zone, and then the intermediate species is oxidized to form the final combustion products.

Moreover, there is a particular peninsula along the left V branch in each flame for both H_2 and CO distributions. This peninsula is similar to that observed by Galizzi in the experiment [9], Fig.2, except that the positions of the peninsula obtained by the simulations are much lower than that in the experiment.

The reason for the formation of this particular peninsula in the distributions of H_2 and CO can be analyzed now. The profiles of the inlet equivalence ratio in Fig. 1b show that the equivalence ratio around x = 0.0 is higher than the stoichiometric value 1.0, and the stabilization rod is located on the right side of x = 0.0. Therefore the mixture in the left near stabilization rod region is fuel rich. When the fuel rich mixture enters the primary reaction zone, the parent fuel is fully converted to some intermediate species, such as H_2 and CO, in the V-shaped primary reaction zone. However, due to the shortage of oxygen, the intermediate species H_2 and CO formed in the left V branch near the stabilization rod can be further diffused toward the middle of the V-shaped fuel-free region. Therefore the particular peninsula is formed. Moving to the downstream, the intermediate species like H_2 and CO in the peninsula are gradually converted to combustion products by the reaction with oxygen penetrating from the fuel lean region (right V-branch and downstream of left V-branch).

The concentrations of oxygen in the three simulated flames are shown in Fig. 6. It is found that although oxygen concentration starts to decrease from the two V branches, it can appear in most of the V-shaped fuel-free zone, except in the small region where the H_2 or CO peninsula locates. In the small peninsula region, the concentration of oxygen is further reduced or totally vanishes. It is because oxygen is further consumed by H_2 and CO. Therefore we can call the peninsula region as a diffusion flame branch where the H_2 and CO formed in the left fuel rich V-branch region is converted to combustion products by the reaction with oxygen. This region is different from the primary reaction zone along the two V branches, where fuel and oxygen are premixed. It should be point out that because the fuel rich (equivalence ration greater than 1.0) region at the inlet is very narrow in the simulations, the peninsula regions are very small in all the three simulated flames. Consequently the reaction intensity and the heat release rate in the peninsula region are much smaller than in the primary V-shaped reaction zone. This is the reason that we cannot observe a significant heat release region inside the two primary V branches.

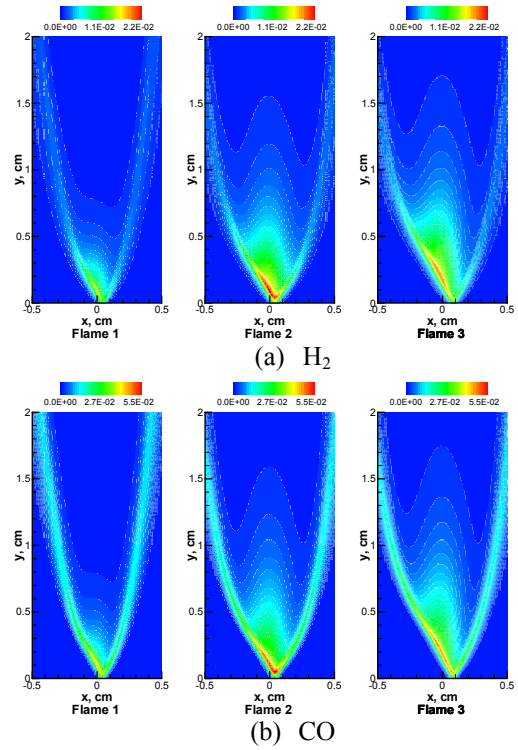

Fig. 5 Mole fractions of H_2 and CO in the simulated flames.

As mentioned in the numerical model section, the flame conditions in the simulations are different from in the experiment [9]. The main difference is the flame dimension. The dimension in the simulations is only one fifth as in the experiment. As a result, everything, except for the inlet temperature, in Flame 1 was reduced to one fifth as in the experiment. The width of fuel rich region, the rod diameter and the distance between the rod and x = 0.0 in Flame 1 are only one fifth of those in Galizzi's experiment [9]. In Flame 2, all the conditions are the same as those in Flame 1, but the width of fuel rich region (see Fig. 1b) doubles, compared to Flame 1. The other conditions of Flame 3 are the same as in Flame 2, except the distance between the rod and x = 0.0 becomes 0.8 mm.

Comparing the results of the three simulated flames, it is noted that the peninsula in Flame 2 is bigger than in Flame 1, and the position of the peninsula on the left V-branch in Flame 3 is higher than in Flame 2. The narrower fuel rich region in Flame 1 causes less H_2 and CO to be formed in the left V-branch. Therefore the peninsula in Flame 1 is smaller than in Flame 2. As for Flames 2 and 3, the difference between them is the distance between the rod and the fuel rich region (x = 0.0). With the rod moving further away from the fuel rich region, the fuel rich region on the left V branch becomes further away from the flame base. Consequently the position of the peninsula in Flame 3 is higher than that in Flame 2.

From the comparison of the three simulated flames, we can infer that with the width of the fuel rich region at the inlet and the distance between the rod and x = 0.0 further increasing to close to the experimental conditions, the peninsula size will be increased and the position of it will become higher than in the

three simulated flames of this paper. We expect that if we could exactly simulate the experimental flame in [9], the peninsula in the distributions of H_2 or CO will be very close to the particular shape observed on the left V-branch by the experiment, as shown in Fig. 2. Therefore we can conclude that the particular peninsula observed by Galizzi in the experiment is caused by the formation of a diffusion flame where intermediate species, like H_2 and CO, react with oxygen penetrating from the primary V-shaped reaction zone.

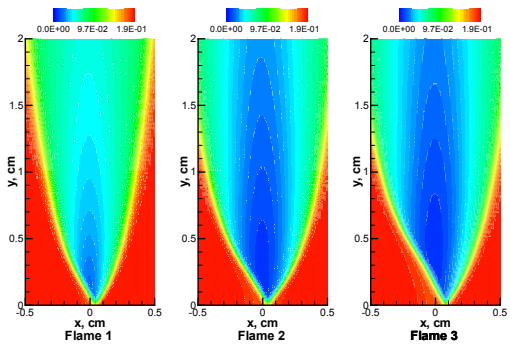

Fig. 6 Mole fraction of O_2 in the simulated flames.

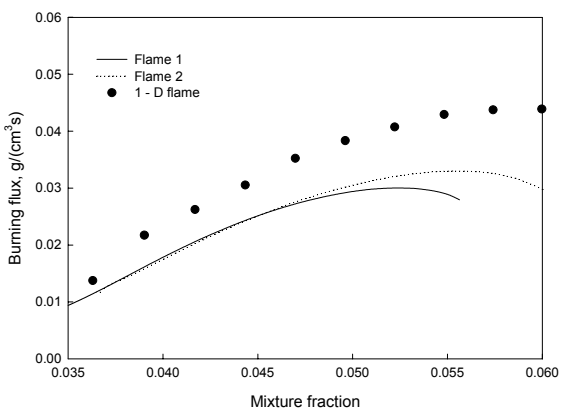

Fig. 7 Local burning flux on the left V-branch.

Due to the variation in equivalence ratio, an interesting property for a stratified flame is the local burning flux, the product of local flame propagation speed and density, along the primary premixed reaction surface. For the flames studied in this paper, this surface is along the V-shaped primary reaction zone. There are multiple definitions for flame speed. Although some researchers argued that the consumption speed is more meaningful to represent the burning velocity, it is difficult to obtain the local value in multi-dimensional flames. The displacement speed is used in this paper. Generally it can be obtained by equating the transport equation for a scalar variable with the Hamilton-Jacobi equation for the scalar field [17]. For a steady state simulation, this property can be simply obtained by evaluating the local fluid velocity normal to the flame surface.

A difficulty in calculating the displacement speed is to locate the flame surface. As a flame has a finite thickness, there is some ambiguity in selecting this surface. In our previous study on triple flames, the contour line with the CO_2 mole fraction of 0.04 was found to be reasonable to represent the envelopes of a triple flame. This method was also used in this paper. We chose the burning flux, rather than the speed, to reflect the burning intensity, since it is affected mainly by the variation of the stream tube area, while the speed is affected by the variations in both the stream tube area and the temperature.

Figure 7 shows the local flux versus mixture fraction [18] for Flames 1 and 2. For comparison, the burning flux of one-dimensional planar premixed CH_4/air flame, obtained from reference 15, is also given. Only the burning fluxes on the left V-branch are displayed, since the peninsula appears on it. The burning flux of Flame 3 is not shown, because its stabilization rod differs from that of Flames 1 and 2. The mixture fraction rather than equivalence ratio was used is owing to the fact that equivalence ratio cannot be calculated inside the reaction zone. Mixture fraction can reflect the fresh mixture composition. The mixture fraction of 0.055 corresponds to the equivalence ratio of 1.0. The smaller the mixture fraction, the leaner the fresh mixture. It is observed that the burning fluxes of both Flames 1 and 2 are smaller than that of the one-dimensional planar premixed flame. The burning flux of Flame 1 in the very lean region is similar to that in Flame 2. However, when the stoichiometric mixture fraction is approached, the burning flux of Flame 2 becomes higher than that of Flame 1.

In a stratified flame, the flame surface is curved and thus the flame is stretched. This leads the lower burning fluxes of Flames 1 and 2 than that of a one-dimensional planar premixed flame [19], for which the stretch rate is zero.

The curvatures of the left V-branches of Flames 1 and 2 are similar, when the mixture fraction is far off the stoichiometric value. Therefore the stretch rates of the left V-branch for the two flames are very close. As a result, no significant difference can be observed for the burning fluxes of Flames 1 and 2 in the very lean region.

With the stoichiometric mixture fraction being approached, the position along the left V-branch is close to the particular peninsula, Fig. 5. More hydrogen and other radicals in the peninsula can diffuse to the left V-branch of the primary reaction zone. This mass diffusion of hydrogen and other radicals intensifies the combustion reactions there. Besides, since the CO and H_2 in the peninsula are further oxidized to the final combustion products, the temperature in the peninsula is higher than in the V-shaped primary reaction zone. Therefore there is also heat transfer from the peninsula to the left V-branch. The heat transfer also enhances the combustion intensity on the left V-branch of the primary reaction zone. As indicated before, the peninsula of Flame 2 is bigger than that of Flame 1. Consequently, the heat transfer and the mass diffusion from the peninsula to the left V-branch are increased in Flame 2, compared to Flame 1. This causes the burning flux of Flame 2 to be higher than that of Flame 1, when the stoichiometric mixture fraction is approached.

We expect that with the increase of the stratified charge region and thus the peninsula, the heat transfer and the mass diffusion from the peninsula will be further intensified. Therefore the formation of the diffusion flame and the interaction of the diffusion flame and the primary premixed flame increase the flame speed of the primary premixed flame. This is a significant feature of a stratified flame.

CONCLUSIONS

A V-shaped laminar stratified flame has been investigated by direct numerical simulation using detailed chemistry and complex thermal and transport properties.

The results indicate that in addition to the primary premixed flame, the stratified charge in a combustor can cause the formation of a diffusion flame within the premixed flame branches. The fuel is fully decomposed and converted to some intermediate species, like CO and H_2, in the primary premixed flame branches. Due to the shortage of oxygen, the formed CO and H_2 in the fuel rich premixed flame region is further diffused to the downstream until they are oxidized by oxygen penetrating from the fuel lean region. This leads to the appearance of the diffusion flame. There is an interaction between the diffusion flame and the primary premixed combustion branch. The interaction intensifies the combustion speed in the primary reaction zone. Both the heat transfer and the mass diffusion of hydrogen and some radicals cause the interaction.

REFERENCES

1. Fan, L., and Reitz, R.D., 2000, "Spray and Combustion Modelling in gasoline direct-injection engines", Atomization and Sprays, Vol. 10, pp. 219-249.
2. Gill, A., Gutheil, E., and Warnatz, J., 1996, "Numerical Investigation of the Combustion Process in a Direct-Injection Charge Engine", Combust. Sci. and Tech., Vol. 115, pp. 317-333.
3. Zhou, J., Nishida, K., Yoshizaki, T., and Hiroyasu, H., 1998, "Flame Propagation Characteristics in a Heterogeneous Concentration Distribution of a Fuel-Air Mixture", SAE paper 982563.
4. Plackmann, J. D., Kim, T., and Ghandhi, J.B., 1998, "The Effects of Mixture Stratification on Combustion in Constant-Volume Combustion Vessel", SAE paper 980159.
5. Phillips, H., 1965, "Flame in a Buoyant Methane Layer", 10th Sym. (Int.) on Combustion, The Combustion Institute, The Combustion Institute, pp.1277-1283.
6. Guo, H., Liu, F., and Smallwood, G.J., 2005, "A Numerical Study of Laminar Methane/Air Triple Flames in Two Dimensional Mixing Layers", submitted to Int. J. Thermal Sciences.
7. Helié, J., Trouvé, A., 1998, "Turbulent Flame Propagation in Partially Premixed Combustion", 27th Sym. (Int.) on Combustion, The Combustion Institute, pp. 891-898.
8. Poinsot, T., Veynante, D., Trouvé, A., and Ruetsch, G., 1996, "Turbulent Flame in Partially Premixed Flames", Proceeding of the Summer Program, Center for Turbulence Research, NASA Ames/Stanford University, pp. 111-136.
9. Galizzi, C., 2003, "Experimental Study of a V-Shaped Flame Stabilized in a Stratified Flow", Ph. D. thesis, Ecole Centrale de Lyon, France.
10. Kuo, K. K., Principles of Combustion, John Wiley & Sons, 1993.
11. Liu, F., Smallwood, G. J., and Gülder, Ö.L., 2000, "Band lumping strategy for radiation heat transfer calculations using a narrowband model", J. Thermophysics Heat Transfer, Vol. 14, pp.278-281.
12. Kee., R.J., Dixon-Lewis, G., Warnatz, J., Coltrin, M.E., and Miller, J.A., A Fortran computer code package for the evaluation of gas-phase, multicomponent transport properties, Report No. SAND 86-8246, Sandia National Laboratories, 1986.
13. Patankar, S.V., Numerical Heat Transfer and Fluid Flow, Hemisphere, New York, 1980.
14. Liu, Z., Liao, C., Liu, C. and McCormick, S., 1995, "Multigrid method for multi-step finite rate combustion", AIAA paper AIAA 95-0205.
15. Smith, G.P., Golden, D.M., Frenklach, M., Moriarty, N.W., Eiteneer, B., Goldenberg, M., Bowman,C.T., Hanson, R.K., Song, S., Gardiner, W.C., Lissianski, J.V.V., and Qin, Z. (1999) http://www.me.berkeley.edu/gri_mech/.
16. Kee, R.J., Dixon-Lewis, G., Warnatz, J., Coltrin, M.E., and Miller, J.A., A fortran computer code package for the evaluation of gas-phase, multicomponent transpotr properties, Report No. SAND 86-8246, Sandia National Laboratories, 1986.
17. Ruetsch, G.R., Vervisch, L., and Liñán, A., 1995, "Effects of Heat Release on triple Flames", Phys. Fluids, Vol. 7, pp.1447-1454.
18. Bilger, R.W., 1988, "The Structure of Turbulent Nonpremixed Flames", Twenty-second Sym. (Int.) on Combustion, The Combustion Institute, pp.475-488.
19. Davis, S.G., Quinard, J., and Searby, G., 2002, "Markstein Numbers in Counterflow, Methane- and Propane- Air Flames: a Computational Study", Combust. Flame, Vol. 130, pp.123-136.